IOSR Journal of Mechanical and Civil Engineering (IOSR-JMCE)
e-ISSN: 2278-1684,p-ISSN: 2320-334X, Volume 13, Issue 5 Ver. VII (Sep. - Oct. 2016), PP 26-32
www.iosrjournals.org

Numerical Approach to Estimate the Effective Yield Surface of Random Porous Media for Spherical Voids

Hanane Elminor, Imane Bahraoui, Hassan Elminor, Elmokhtar Hilali, Toufik Kanit

[1]*Equipe de recherche Matériaux, Mécanique et Génie Civil, ENSA Agadir, Université Ibn Zohr*
[2]*Laboratoire de Mécanique de Lille*

Abstract: *In this paper, we describe a computational homogenization methodology to study of three-dimensional cubic cells in order to estimate the effective yield surface of random porous media containing spheroidal voids. The representativity of the overall yield surface estimates is examined using cubic cells containing randomly distributed. Spherical voids are considered in the computations. The computational results are compared with some existing Gurson-type yield criteria.*

Keywords: *Computational homogenization; Representativity; Random porous media; Gurson-type models.*

I. Introduction

The mathematical development of yield criteria for the plastic porous solids has been widely investigated by Rice and Tracey [1], Gurson [2], Tvergaard [3], Koplik and Needleman [4], Sun and Wang [5], Ponte Castaneda [6], recently by Dunand and Mohr[7], Li et al. [8], Mroginski et al. [9], Fei et al. [10], Shen et al. [11], Yan et al. [12]. The role of porosities regarding the ductile fracture process, these voids being the consequence of manufacturing processes. The mathematical derivations of these criteria are generally based upon the continuum-based micromechanical framework, for which the starting point is the micro structural representation of the porous medium. The non-triviality of the theoretical problem leads to define a basic unit cell containing one centered void for the material volume used to represent the microstructure. The unit cell is an elementary volume element consisting in a hollow sphere or cylinder subjected to a uniform macroscopic strain rate at its external boundary. Gurson [2] proposed the most widely used micromechanics-based yield criterion to analyze plastic porous solids containing spherical voids.

The Gurson model is based upon the following assumptions: isotropy, incompressibility and rigid-plasticity for the local yielding of the surrounding matrix material which obeys to the Von Mises criterion. The resulting macroscopic yield criterion of Gurson [2] for the porous medium is hydrostatic pressure-dependent, integrates the volume fraction of porosities as a model parameter and accounts for a possible void growth driven by the local plastic deformation of the surrounding matrix material. As pointed out by Tvergaard, the Gurson model gives an upper bound of the macroscopic yield stress as a function of the mean stress for a periodic arrangement of voids. In order to improve its agreement with two-dimensional finite element simulation results on a periodic unit cell, Tvergaard [3], proposed to introduce heuristic parameters in the Gurson yield criterion. These adjustable parameters have no direct physical meaning but may be correlated to interaction effects between voids. The extension of the Gurson model by Tvergaard, known as the Gurson-Tvergaard (GT) model, was thenceforth widely used by many researchers to check its capability to capture the poroplastic behavior of many engineering porous materials. In very useful background papers, Benzerga and Leblond [13], and Besson [14], reviewed the various extensions of the Gurson model based upon enhanced micromechanical approaches or upon phenomenological generalizations to take into consideration the void shape or the matrix material features such as isotropic/kinematic hardening, viscoplasticity, compressibility and anisotropy. Using micromechanical approaches, Ponte Castaneda [6] and Sun and Wang [5] proposed, respectively, upper and lower bounds for the overall yield surface of porous media. Using the variational technique introduced by Ponte Castaneda [6] proposed another upper bound which overcomes the well known basic drawbacks of the Gurson criterion at low stress triaxiality values. The effect of void shape on the macroscopic yield response of porous materials was investigated by several authors Gologanu et al. [15], [16], Yee and Mear, [17], recently by Danas and Aravas [18], Madou and Leblond [19], Monchiet and Kondo [20].

Although the mathematical developments have reached a high degree of sophistication, the resulting yield criteria generally involve a certain number of parameters with no physical significance. That may be explained by the fact that these micromechanics-based models consider as material volume element an elementary volume element containing a single void. Because the voids are diluted in the matrix material, the interactions between voids are neglected. Moreover, this microstructural representation of the porous material implies periodicity. However, to be statistically representative, the material volume element should contain sufficient information about the porous microstructure, in particular the void distribution. This last decade, the

material response of porous media was also investigated using computational homogenization. This approach is emerging as a powerful tool to bring a better understanding of void distribution effects and interaction phenomena on the mechanical behavior of random porous media. The main advantage of the computational homogenization is its ability to directly compute the mechanical fields on the random porous media by representing explicitly the microstructure features such as shape, orientation and distribution of voids. Although many studies were dedicated to the development of yield criteria for plastic porous media, it seems that only few works have been devoted to three-dimensional computational homogenization involving multiple voids. To our knowledge, only Bilger et al. [21], Fritzen et al. [22] and Khdir et al. [23] used this approach to estimate the overall yield surface of porous materials. Their computations were limited to spherical voids. The calculations of Bilger et al. [21] were performed on the basis of three-dimensional Fast Fourier Transform. The pore clustering effect on the overall material response was the key point of their investigation. Fritzen et al. [22] assumed the random porous media as a volume of porous material which is periodically arranged. The results highlighted by Fritzen et al. [22] led them to extend the GT yield criterion in order to overcome the analytical/numerical discrepancies. Khdir et al. [22] focused their investigations on the porous materials containing two populations of voids. Their results showed that, for an identical fraction of porosities, there is no significant difference between a double and a single population of voids.

In this contribution, a computational homogenization of random porous media, including spherical voids, is presented in order to determine their overall yield surface while still studying the representativity of the computational results.

II. Homogenization Approach

2.1 Porous microstructures

The porous media considered in the computations are made of perfectly-plastic matrix obeying to the commonly used isotropic Von Mises yield criterion, the yield stress being constant and equal **to 290 MPa**. The plastic flow is assumed perfect in order to disregard hardening effects in the investigation and to compare the simulation results with the most common analytical models. The matrix material is sufficiently stiff in order to overcome any yield strain effects.

The porous media are represented by three-dimensional cubic cells containing a large number of pores, in order to assure that the studied material volume element is sufficiently large compared to porosities. The voids are randomly distributed and oriented in space in the cubic cell. Moreover, they are identical and non-overlapped. The question of the void content effects is examined in this work. The volume fraction of n spheroidal voids inside a cubic cell of volume V is given by:

$$f_{\text{spheroidal}} = \frac{4}{3}\frac{n\pi abc}{V} \qquad (1)$$

where a is the polar radius along the *y* axis of the spheroidal void and, b and c are the equatorial radii along the *z* and *x* axis, respectively.

Three void volume fractions *f* are studied *f* = 0.05, 0.13 and 0.23.

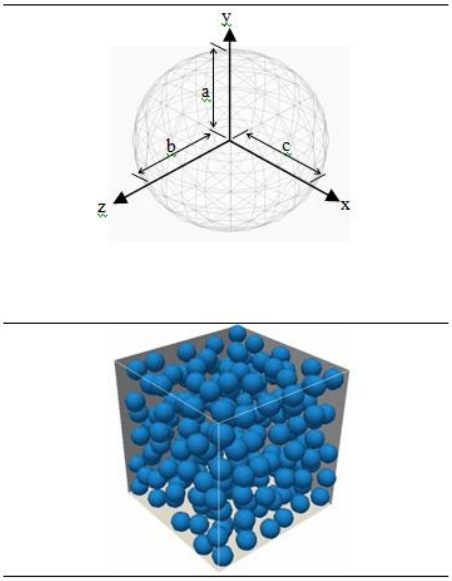

Fig. 1 Examined porous media spherical ($a = b = c$) pore (n ≈ 200 pores)

The void shape effects are examined in this work which constitutes a noteworthy difference with respect to existing literature (Bilger et al. [21] Fritzen et al. [22]; Khdir et al. [23]).

Fig.1 presents the designed porous microstructures. The cases of spherical ($a = b = c$), oblate ($b = c$ and $b > a$) and prolate ($b = c$ and $a > b$) pores are examined. For each shape, three void volume fractions *f* are studied (*f* = 0.05, 0.13 and 0.23). The finite element method was chosen for the numerical computations using *Zebulon* software. A standard small-strain approximation was used for the simulations. The mesh size used was fine enough to represent accurately the geometry of the porosity and to ensure the overall response convergence.

2.2 Boundary conditions

The porous media being hydrostatic pressure-dependent, the boundary conditions imposed to the designed representative element should involve a wide range of stress trriaxiality ratios to be explored. The stress triaxiality parameter $T = \Sigma_m / \Sigma_{eq}$ is defined as the ratio of the overall hydrostatic stress Σ_m and the overall Von Mises equivalent stress Σ_{eq}, respectively, given by:

$$\Sigma_m = \frac{1}{3} tr(\mathbf{\Sigma}) \text{ and } \Sigma_{eq} = \sqrt{\frac{3}{2}} (\mathbf{\Sigma}' : \mathbf{\Sigma}')^{1/2} \quad (2)$$

where $\mathbf{\Sigma}$ is the macroscopic stress tensor and $\mathbf{\Sigma}'$ denotes its deviatoric part.

In this work, due to its computational robustness, the following mixed boundary conditions were imposed:

$$\begin{aligned} E_{11}(t) &= t\dot{\varepsilon}_0(\alpha + \beta) \\ E_{22}(t) &= t\dot{\varepsilon}_0(-\alpha + \beta) \\ E_{33}(t) &= t\dot{\varepsilon}_0\beta \\ \Sigma_{12}(t) &= \Sigma_{13}(t) = \Sigma_{23}(t) = 0 \end{aligned} \quad (3)$$

In which the values assigned to shear components of the overall stress tensor are zero. The terms *α* and *β*, introduced to control the diagonal components of the overall strain tensor $\mathbf{E}$, are two loading parameters, $\dot{\varepsilon}_0 > 0$ is a prescribed deformation rate and *t* is the simulation time. The stress triaxiality is indirectly assigned by the two measures of stress, given by Eq. (3.14), which are defined implicitly by the mixed boundary conditions through the two loading parameters *α* and *β*. The different values of *α* and *β* used to obtain different stress triaxiality ratios are listed in Table1.

	1	2	3	4	5	6	7	8	9
α	1.00	1.00	1.00	1.00	1.00	1.00	1.00	0.50	0.00
β	0.00	0.05	0.10	0.15	0.25	0.50	1.00	1.00	1.00

Table 1. Loading parameters used in the simulations.

III. Results And Discussion

3.1 Representativity (RVE)

The size of the volume element is conditioned by the number of porosities which should be chosen large enough to ensure that the volume element is representative. This representativity was investigated in terms of the mechanical responses by Huet [26], Drugan and Willis [25] and Kanit et al. [27]. These authors have studied the effects of the volume element size on the elastic stiffness. More recently, Khdir et al. [23] have investigated these effects on the elastic-plastic response. In the case of elastic-plastic composites, made of two phases with highly contrasted properties, Khdir et al. [23] have shown that the minimum size of the volume element in the yield and post-yield region must be greater than the minimum size required in the elastic domain. This question which arises in three-dimensional computational homogenization has to be systematically accounted for. Several volume elements with different sizes (i.e. containing different number of pores) are simulated for a porosity of *f= 0.23*, and the mechanical representativity of the computational results are examined. The overall stationary stresses are plotted as a function of the number of pores in Fig. 2 for the three shapes.

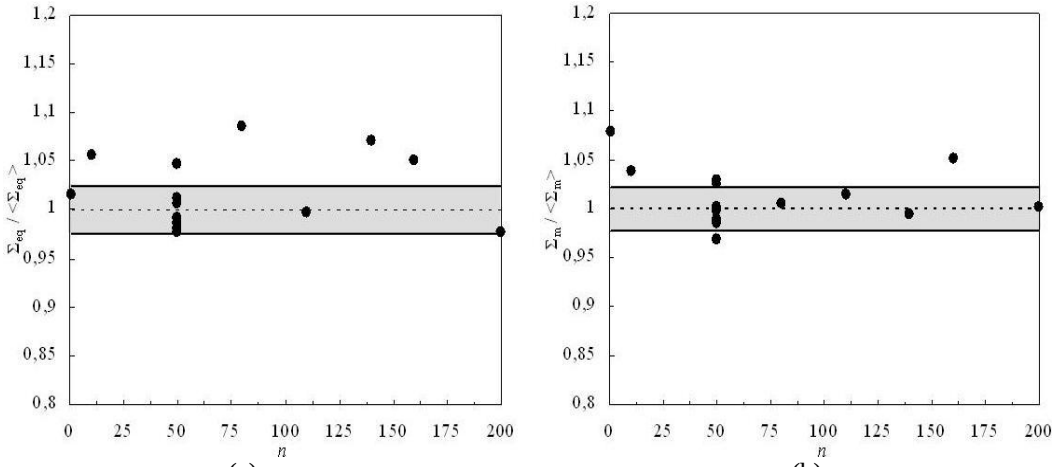

Fig. 2 Asymptotic overall Von Mises equivalent stress and hydrostatic stresses as a function of the number of pores for spherical pores at $f = 0.23$ The average (dashed line) and the standard deviations (colored area) are calculated for $n = 50$.

Figs. 2 a correspond to the loading path 1 in Table 1 characterized by ($\alpha = 1$, $\beta = 0$) for which the deviatoric component exhibits the highest stationary value, whereas Figs. 2 b correspond to the loading path 9 in Table 1 characterized by ($\alpha = 0$, $\beta = 1$) for which the hydrostatic component takes its highest stationary value. The stationary stresses are normalized with respect to the average value of computational results of several realizations containing 50 pores. All computed data are found within or close to the colored area defined by the standard deviations. The stationary values for $n = 200$ are close to the averages of $n = 50$ pores, the largest difference being about 7%. The computations are performed using the largest cubic cells (containing $n = 200$ voids) in order to assure the mechanical representativity of the numerical yield surfaces.

These cubic cells are successively stretched in the orthogonal directions. It can be observed that identical overall mechanical responses are obtained which is, for isotropy, a necessary condition but not sufficient. To ensure this property the cubic cells must also be subjected to simple shear loading. We observed that the overall shear responses are the same in three perpendicular planes. Then, when a sufficient number of pores are randomly distributed and oriented in the volume element, an isotropic response is obtained at the macroscopic scale. The found isotropy proves that this large volume element is representative enough of the random porous medium, whatever the void shape.

3.2 Local plastic strain fields

The local plastic strain fields can be observed in Fig.3 at different triaxiality ratios for spherical pores. The porosity of $f = 0.23$ is chosen to illustrate this distribution. The observations are presented at the end of the prescribed loading. The pore-pore interactions and the triaxiality effects on the local fields are illustrated in the figures for three particular cases: The cases ($\alpha = 1$, $\beta = 0$) and ($\alpha = 0$, $\beta = 1$) correspond to the lowest and highest triaxiality ratios, respectively, and the case ($\alpha = 1$, $\beta = 0.25$) to an intermediate one.

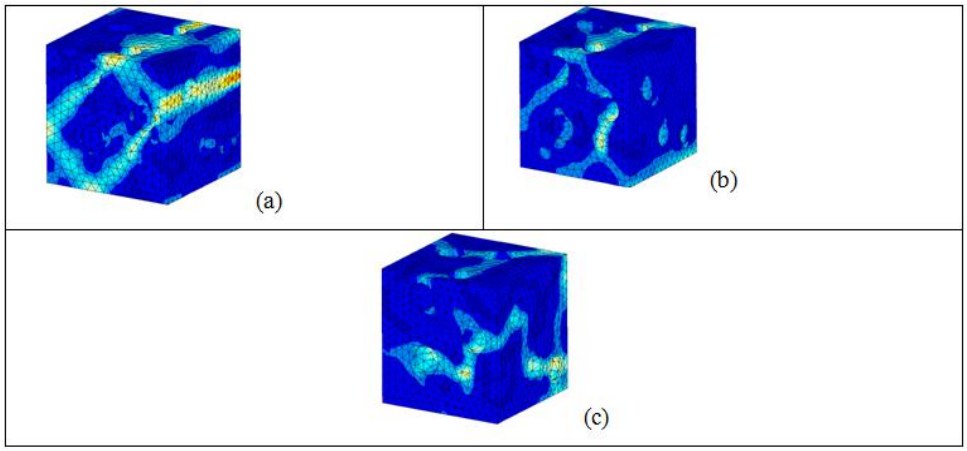

Fig. 3 Distribution of the accumulated plastic strain for spherical pores at $f = 0.23$ and three different loading cases: (a) $\alpha = 1$, $\beta = 0$, (b) $\alpha = 1$, $\beta = 0.25$, (c) $\alpha = 0$, $\beta = 1$.

3.3 Comparison between numerical results and analytical criteria

In this subsection, the case of spherical pores is analyzed. The common representation of the overall yield surface, plotting the overall Von Mises equivalent stress as a function of the overall hydrostatic stress, is adopted to illustrate the computational data.

The computed data are compared with some existing analytical models in Figs.4, 5, 6 for the three considered void volume fractions. Besides the commonly used Gurson model, other analytical models are selected. The mathematical expressions of some existing yield criteria for plastic porous materials are recalled in Table 2.

G yield criterion (Gurson [2], 1977)	$\Phi(\boldsymbol{\Sigma}, f)=\frac{\Sigma_{eq}^2}{\sigma_0^2}+2f\cosh\left\{\frac{3}{2}\frac{\Sigma_m}{\sigma_0}\right\}-1-f^2=0$	(4)
GT yield criterion (Tvergaard [3], 1981)	$\Phi(\boldsymbol{\Sigma}, f)=\frac{\Sigma_{eq}^2}{\sigma_0^2}+2q_1 f\cosh\left\{\frac{3}{2}q_2\frac{\Sigma_m}{\sigma_0}\right\}-1-q_3 f^2=0$	(5)
PC yield criterion (Ponte Castañeda [6], 1991)	$\Phi(\boldsymbol{\Sigma}, f)=\left(1+\frac{2}{3}f\right)\frac{\Sigma_{eq}^2}{\sigma_0^2}+\frac{9}{4}f\frac{\Sigma_m^2}{\sigma_0^2}-(1-f)^2=0$	(6)
GS yield criterion (Gărăjeu and Suquet [24], 1997)	$\Phi(\boldsymbol{\Sigma}, f)=\left(1+\frac{2}{3}f\right)\frac{\Sigma_{eq}^2}{\sigma_0^2}+2f\cosh\left\{\frac{3}{2}\frac{\Sigma_m}{\sigma_0}\right\}-1-f^2=0$	(7)
SW yield criterion (Sun and Wang [5], 1989)	$\Phi(\boldsymbol{\Sigma}, f)=\frac{\Sigma_{eq}^2}{\sigma_0^2}+f\left(2-\frac{1}{2}\ln f\right)\cosh\left\{\frac{3}{2}\frac{\Sigma_m}{\sigma_0}\right\}-1-f(1+\ln f)=0$	(8)

Table 2. Gurson-type yield criteria

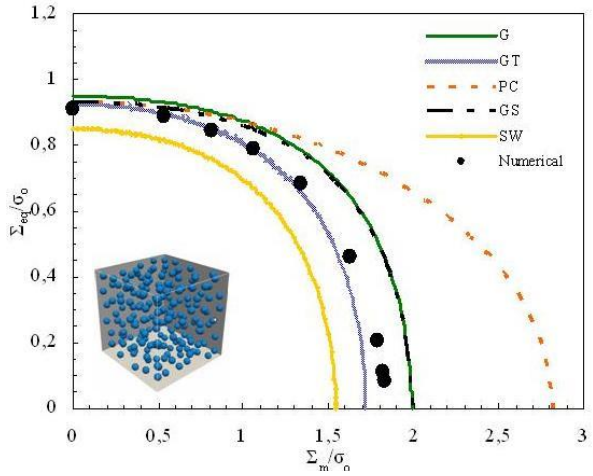

Fig. 4 Comparison between some existing analytical models and the simulation results for spherical pores at $f = 0.05$, $n \approx 200$ pores

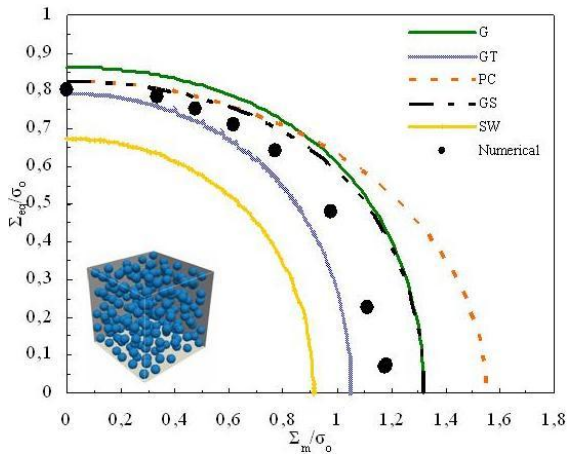

Fig. 5 Comparison between some existing analytical models and the simulation results for spherical pores at $f = 0.13$, $n \approx 200$ pores

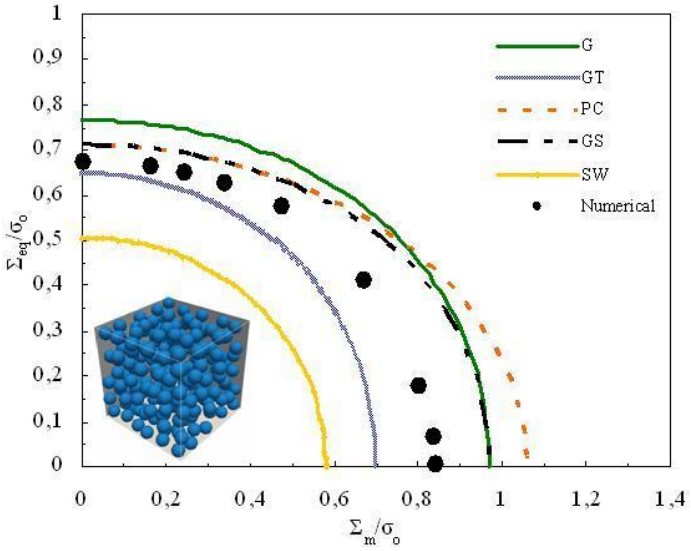

Fig.6 Comparison between some existing analytical models and the simulation results for spherical pores at $f = 0.23$; $n \approx 200$ pores

It can be observed in that the computed data satisfy the Gărăjeu and Suquet [24] upper bound and the Sun and Wang [5] lower bound. The GS model is identical to the Gurson model around the normalized hydrostatic stress axis and to the Ponte Castaneda [6] model around the normalized equivalent stress axis. Around the normalized hydrostatic stress axis, the GS model is identical to the Gurson model, but strongly deviates when decreasing the mean stress axis. It can be observed that the GS model overestimates the numerical data for high normalized hydrostatic stress, but becomes closer when decreasing the mean stress.

All the computed data satisfy the SW lower bound but it is found that the SW model is close to the numerical data around the normalized equivalent stress axis at the lowest void content. The PC yield criterion provides too stiff predictions around the normalized hydrostatic stress axis. The divergences with the model decrease when the void content increases. The G criterion overestimates the numerical data, the difference between the two solutions increasing with the void content. The GT model using the calibrated parameters of Tvergaard [3], see Table 2, underestimates the numerical yield surface. For the lowest void content, the GT model is close to the numerical surface, especially around the normalized equivalent stress axis. For the highest void content, the GT model becomes a lower bound.

IV. Conclusion

The overall yield surface of plastic porous media was investigated via computational micromechanics. The computational results were investigated in terms of representativity and were related to some existing Gurson-type yield criteria for spherical voids. We have found that the Gurson-Tvergaard heuristic parameters are independent on the void size which could suggest that a porous medium containing a single population of voids could properly represent a same medium with two populations of voids.

V. References

[1]. Rice, J.R., Tracey, D.M., On the ductile enlargement of voids in triaxial stress fields. *Journal of the Mechanics and Physics of Solids 17*, 201-217.
[2]. Gurson, A.L., Continuum theory of ductile rupture by void nucleation and growth: Part I - Yield criteria and flow rules for porous ductile media. *Journal of Engineering Materials and Technology*, 1977, 99, 2-15.
[3]. Tvergaard. V., Influence of voids on shear band instabilities under plane strain conditions. *International Journal of Fracture 17*, 1981, 389-407.
[4]. Koplik, J., Needleman, A., Void growth and coalescence in porous plastic solids. *International Journal of Solids and Structures 24*, 1988, 835-853.
[5]. Sun, Y., Wang, D., A lower bound approach to the yield loci of porous materials. *Acta Mechanica* 5, 1989, 237-243
[6]. Ponte Castañeda, P., The effective mechanical properties of non-linear isotropic composites. *Journal of the Mechanics and Physics of Solids 1*, 1991, 45-71
[7]. Dunand, M., Mohr, D., On the predictive capabilities of the shear modified Gurson and the modified Mohr-Coulomb fracture models over a wide range of stress triaxialities and Lode angles. *Journal of the Mechanics and Physics of Solids 59*, 2011, 1374-1394.
[8]. Li, Z., Huang, M., Combined effects of void shape and void size - oblate spheroidal microvoid embedded in infinite non-linear solid. *International Journal of Plasticity 21*, 2005, 625-650.
[9]. Mroginski, J.L., Etse, G., Vrech, S.M., A thermodynamical gradient theory for deformation and strain localization of porous media. *International Journal of Plasticity 27*, 2011, 620-634.

[10]. Fei, H., Yazzie, K., Chawla, N., Jiang, H., The effect of random voids in the modified gurson model. *Journal of Electronic Materials 41*, 2012, 177-183.

[11]. Shen, W., Shao, J.F., Dormieux, L., Kondo, D., Approximate criteria for ductile porous materials having a green type matrix: application to double porous media. *Computational Materials Science 62*, 2012, 189-194

[12]. Yan, Y., Sun, Q., Chen, J., Pan, H., The initiation and propagation of edge cracks of silicon steel during tandem cold rolling process based on the Gurson-Tvergaard-Needleman damage model. *Journal of Materials Processing Technology 213*, 2013, 598-605.

[13]. Benzerga, A., Leblond. J.B., Ductile fracture by void growth to coalescence. *Advances in Applied Mechanics 44*, 2010, 169-305.

[14]. Besson, J., Continuum models of ductile fracture: a review. *International Journal of Damage Mechanics 19*, 2010, 3-52.

[15]. Gologanu, M., Leblond, J.B., Perrin, G., Devaux, J., Recent extensions of Gurson's model for porous ductile metals. In: Suquet, P. Editor, *Continuum Micromechanics. Berlin: Springer-Verlag*, 1997, pp. 61-130.

[16]. Gologanu, M., Leblond, J.B., Perrin, G., Devaux, J., Theoretical models for void coalescence in porous ductile solids. I. Coalescence "in Layers". *International Journal of Solids and Structures 38*, 2001, 5581-5594.

[17]. Yee, K.C., Mear, M.E., Effect of void shape on the macroscopic response of non-linear porous solids. *International Journal of Plasticity 12*, 1996, 45-68.

[18]. Danas, K., Aravas, N., Numerical modeling of elasto-plastic porous materials with void shape effects at finite deformations. *Composites: Part B 43*, 2012, 2544-2559.

[19]. Madou, K., Leblond, J.B., A Gurson-type criterion for porous ductile solids containing arbitrary ellipsoidal voids. I: Limit-analysis of some representative cell. *Journal of the Mechanics and Physics of Solids 60*, 2012, 1020-1036.

[20]. Monchiet, V., Kondo, D., Combined voids size and shape effects on the macroscopic criterion of ductile nanoporous materials. *International Journal of Plasticity 43*, 2013, 20-41.

[21]. Bilger, N., Auslender, F., Bornert, M., Moulinec, H., Zaoui, A., Bounds and estimates for the effective yield surface of porous media with a uniform or a nonuniform distribution of voids. *European Journal of Mechanics A/Solids 26*, 2007, 810-836.

[22]. Fritzen, F., Forest, S., Böhlke, T., Kondo, D., Kanit, T., Computational homogenization of elasto-plastic porous metals. *International Journal of Plasticity 29*, 2012, 102-119.

[23]. Khdir, Y.-K., Kanit, T., Zaïri, F., Naït-Abdelaziz, M., Computational homogenization of elastic-plastic composites. *International Journal of Solids and Structures 50*, 2829-2835.

[24]. Gărăjeu, M., Suquet, P., Effective properties of porous ideally plastic or viscoplastic materials containing rigid particles. *Journal of the Mechanics and Physics of Solids 45*, 1997, 873-902.

[25]. Drugan, W.J., Willis, J.R., 1996. A micromechanics-based nonlocal constitutive equation and estimates of representative volume element size for elastic composites. Journal of the Mechanics and Physics of Solids 44, 497-524.

[26]. Huet, C., 1990. Application of variational concepts to size effects in elastic heterogeneous bodies. Journal of the Mechanics and Physics of Solids 38, 813-841.

[27]. Kanit, T., Forest, S., Galliet, I., Mounoury, V., Jeulin, D., 2003. Determination of the size of the representative volume element for random composites: statistical and numerical approach. International Journal of Solids and Structures 40, 3647-3679.